

1961

## Crystallite-Size Determination of MgO by X-Ray Diffraction Line Broadening

E. A. Rosauer  
*Iowa State University*

R. L. Handy  
*Iowa State University*

*Let us know how access to this document benefits you*

Copyright ©1961 Iowa Academy of Science, Inc.

Follow this and additional works at: <https://scholarworks.uni.edu/pias>

---

### Recommended Citation

Rosauer, E. A. and Handy, R. L. (1961) "Crystallite-Size Determination of MgO by X-Ray Diffraction Line Broadening," *Proceedings of the Iowa Academy of Science*, 68(1), 357-371.

Available at: <https://scholarworks.uni.edu/pias/vol68/iss1/53>

This Research is brought to you for free and open access by the IAS Journals & Newsletters at UNI ScholarWorks. It has been accepted for inclusion in Proceedings of the Iowa Academy of Science by an authorized editor of UNI ScholarWorks. For more information, please contact [scholarworks@uni.edu](mailto:scholarworks@uni.edu).

**Offensive Materials Statement:** Materials located in UNI ScholarWorks come from a broad range of sources and time periods. Some of these materials may contain offensive stereotypes, ideas, visuals, or language.

# Crystallite-Size Determination of MgO by X-Ray Diffraction Line Broadening<sup>1</sup>

E. A. ROSAUER AND R. L. HANDY<sup>2</sup>

**Abstract.** The Scherrer equation which relates the pure diffraction breadth to crystallite size of the diffracting substance is applied to a study of various heat-treated MgO powders. A statistical treatment is used to examine effects of sample preparation and the diffraction system and to determine the degree of accuracy of the method. The procedure as described should give a relative accuracy in the 10,000 Å range of  $\pm 10$  percent, and measurements may be made to 100,000 Å.

Comparison of the X-ray data with electron micrographs indicated that the latter gave information with regard to aggregate, not crystallite size. Aggregates grow only slightly with increased temperature treatment. Within the aggregates, individual crystallites grow moderately to 600°C, then greatly increase in size with increased temperature to 1600°C. Low temperature treated MgO has a dilated unit cell which tightens to a constant value after treatment to about 1000°C.

X-ray diffraction is useful not only for identifying chemical constituents in various commercial limes (Table 1), but also for determining size and shapes of individual crystallites of these compounds. Identification is now routine on the basis of d-spacings in the sample, and a qualitative analysis can be made in a few minutes, but crystallite sizes are obtained less directly from width of the diffraction peaks. A narrow, sharp peak indicates relatively coarse material, and a low, broad, peak indicates fine crystallites ultimately transitional to an amorphous phase (Figure 1).

Table 1. Chemical Constituents of Commercial Lime

Source rock	Limestone, CaCO <sub>3</sub>	Dolomite, CaMg(CO <sub>3</sub> ) <sub>2</sub>
Quicklime	CaO	CaO + MgO
Hydrated lime	Ca(OH) <sub>2</sub>	Ca(OH) <sub>2</sub> + MgO, (monohydrate), or Ca(OH) <sub>2</sub> + Mg(OH) <sub>2</sub> (dihydrate)

The X-ray diffraction line broadening technique is ordinarily used for measurements in the size ranges 15 to 2,000 Å (0.00015 to 0.2 micron), or approximately the range covered by the electron microscope. Though the electron microscope gives the advantage of direct observation of size, the X-ray method is faster and statistically more valid because it measures a far greater number of grains. A disadvantage of the X-ray method

<sup>1</sup> A report of the Iowa Engineering Experiment Station project 340-S sponsored by the Iowa Highway Research Board, HR-48, and the Iowa State Highway Commission.

<sup>2</sup> Assistant Professor and Associate Professor of Civil Engineering, respectively, Iowa Engineering Experiment Station, Iowa State University, Ames.

is that it is indirect, and may be inaccurate so far as absolute determination of size although at the same time it is quite accurate for comparative determinations.

It is expected that crystallite sizes in commercial limes will correlate with their physical and chemical properties, for example inactivity as a result of "dead-burning." This paper reports the first phase of the investigations—evolution of technique and apparatus for accurate size determinations of one component of commercial limes.

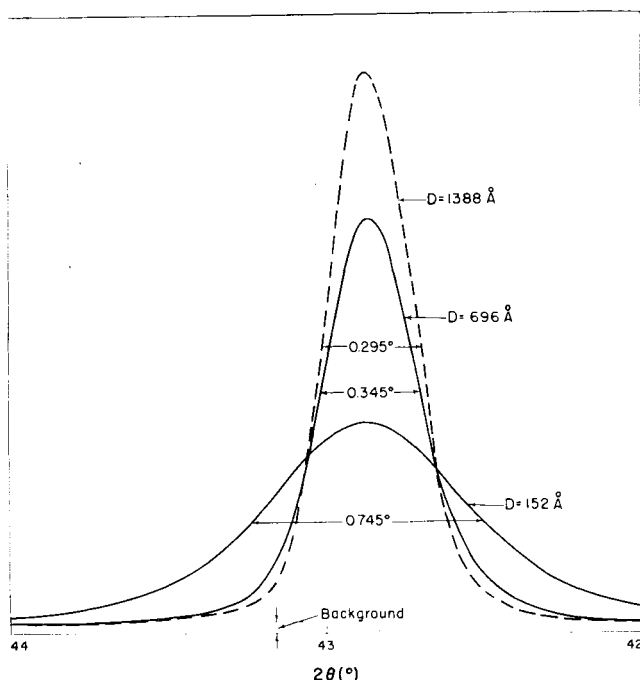


Figure 1. Relation between line broadening of MgO (200) peak and crystallite size.

### THE PHENOMENON OF LINE BROADENING

The Bragg equation,  $\sin \theta = \frac{n\lambda}{2d}$ , specifies a definite angle for

a diffraction maximum to occur, the angle  $\theta$  between an atomic plane in a crystal, and the incident X-ray beam. The incident beam is diffracted from different planes in phase, i.e. the difference in the path length of the diffracted beam is an integral multiple of one wavelength. In large crystals containing numerous parallel atomic planes the value of  $\theta$  is very precise, and the diffraction maximum is sharp.

In small crystals or crystallites the number of atomic planes is reduced, and a small deviation from the ideal  $\theta$  angle becomes tolerable to in-phase diffraction. The diffraction therefore no longer produces a sharp maximum. The normally sharp diffraction peak broadens, the amount of broadening is related to size of the crystallite.

This equation was quantitatively defined by Scherrer (1918) with the equation

$$D = \frac{K\lambda}{\beta \cos \theta},$$

which relates the mean dimension,  $D$ , normal to the diffracting planes of the crystals to the pure diffraction broadening,  $\beta$  is usually defined as the peak breadth in radians at half-maximum peak height (Figure 1). The quantity  $K$  is a constant, given values ranging from 0.70 to 1.70 by various investigators, depending on several factors, including crystal shape. Because the shape may vary within the same sample as well as between samples, one practice is to set  $K$  equal to unity (Klug and Alexander, 1954, p. 511). This has the advantage of making published data comparable.

#### EVALUATION OF THE PURE DIFFRACTION BREADTH, $\beta$

The experimentally observed diffraction peak breadth,  $\beta$ , must be corrected for errors arising in its production and measurement.

##### *Broadening Due to $K\alpha_1\alpha_2$ Doublet*

The  $K\alpha$  radiation commonly used for X-ray diffraction does not consist of a single wavelength but of two very closely spaced wavelengths,  $K\alpha_1$  and  $K\alpha_2$ , which cause broadening of the diffracted beam profile. At low Bragg angles the angular separation of  $\alpha_1$  and  $\alpha_2$  diffractions, here designated  $\Delta$ , is small, and the diffraction peak represents a sum of the two diffractions (*top*, Figure 2). At large  $2\theta$  values or where broadening due to the other factors is small, the angular separation of the doublet may be so resolved (*bottom*, Figure 2) that it is possible to measure the  $K\alpha_1$  peak alone and no correction is necessary.

Generally, the measurement of broadening at half-maximum intensity includes both  $\alpha_1$  and  $\alpha_2$ . Because the  $\alpha_1$  and  $\alpha_2$  diffraction breadths are not linearly additive, curves or equations may be used to correct line breadths for  $K\alpha$ -doublet broadening. The relationship used in this paper is shown on the left in Figure 3 (Klug and Alexander, 1954, p. 504).

The angular separation of the  $K\alpha_1\alpha_2$  doublet,  $\Delta$ , can be ap-

proximated from the Internationale Tabellen (1935), but may be found more accurately through use of the following equation:

$$\Delta = \frac{360}{\pi} \frac{\lambda\alpha_2 - \lambda\alpha_1}{\lambda_{av}} \tan \theta_{av} = C \tan \theta.$$

Derivation of the equation and representative values for C are given in Appendix A.

Calculation of the corrected broadening B from measured breadth  $B_0$  and angular separation  $\Delta$  is illustrated in 1, Appendix B.

*Broadening Due to the Instrument*

The X-ray diffractometer gives great advantage over film methods for crystallite-size measurements because of the speed and the precision of the technique. Because the X-ray beam is not infinitesimally thin, and because of horizontal and vertical beam divergence and other factors such as penetration of the beam into the sample, instrument geometry contributes to broadening of the diffracted line profile. The amount of broadening depends on the X-ray optics employed and on the sample. In addition the electronic circuitry, in particular the time constant of the apparatus used in measuring the counting rate, contributes to the broadening.

The usual procedure in correcting for instrument broadening

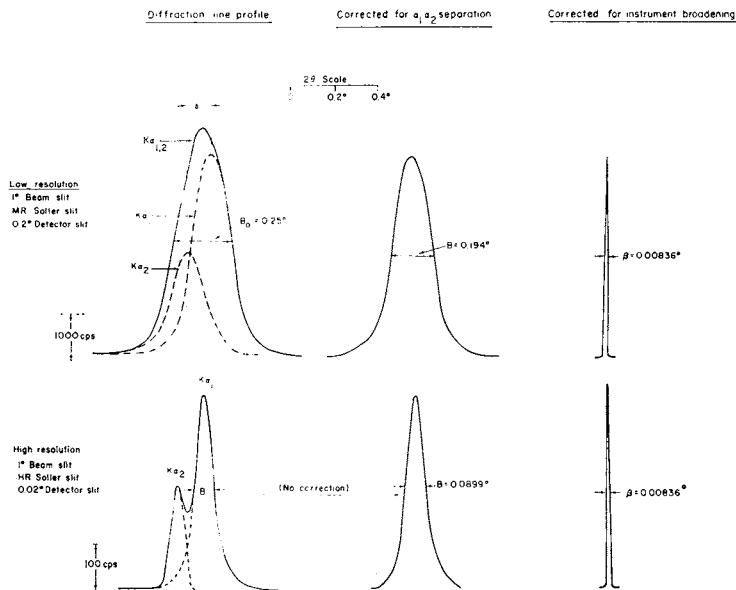


Figure 2. Schematic corrections of the observed line profile for broadening due to  $K\alpha_{1,2}$  doublet and instrument geometry.

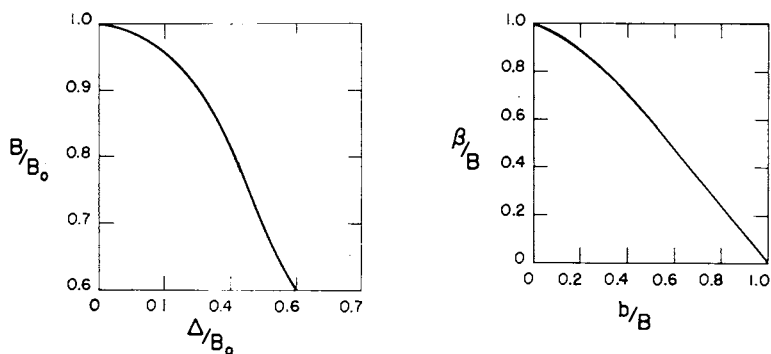


Figure 3. Curves for correcting line breadths for  $\alpha_1\alpha_2$  broadening (left) and instrument broadening (right).

is to adopt a geometry and time constant and determine the diffraction line breadth of a "coarse" material, such that broadening due to small crystallite size and lattice distortion is at a minimum. The line breadth still contains broadening due to the  $K\alpha_1\alpha_2$  doublet, which must be corrected for. After this correction, the value obtained is designated as  $b$ , and represents breadth due purely to instrument factors. As in the  $\alpha_1\alpha_2$  separation, instrument broadening must be subtracted from measured breadths of the material whose size is sought, but again the breadths are not directly additive, and curves are used for the correction (right, Figure 3) (Klug and Alexander, 1954, p. 508). Relation of instrument broadening to diffractometer geometry may be seen by comparing the top and bottom graphs of Figure 2. An example calculation is given in Appendix B.

Ordinarily the "coarse" material chosen for reference is coarser than 1000 Å (0.1 micron), such that broadening due to small crystallite size is near minimum. Often material in the size range 0.5 to 1 micron is used. For the present study large single crystals of  $MgO^3$  were crushed, dry ball-milled, and separated by air elutriation and by sieving. Measurable line broadening was found with material even in the 20 to 44 micron size range, perhaps because of incomplete size separation. Sieved material 44 to 53 microns in size was used and X-rayed ten times to obtain statistical validity.

#### DIFFRACTION SYSTEM

##### Sample Holder

The X-ray diffraction unit is a G. E. XRD-5 utilizing horizontal instrument geometry and vertically-mounted samples. Initial repetitive tests with powders mounted in standard rectangular

<sup>3</sup> Norton Company optical grade Magnorite.

sample holders showed considerable variation in diffraction peak breadth when the holder was shifted between runs. To facilitate this movement a disc-shaped sample holder was adopted so that the sample might be quickly rotated a random amount between runs. Disc sample holders are nominal 1/2-inch brass washers, 1.25 inch o.d. and 0.091 inch thick, with the center drilled out to 3/8 inch diameter (Figure 4).

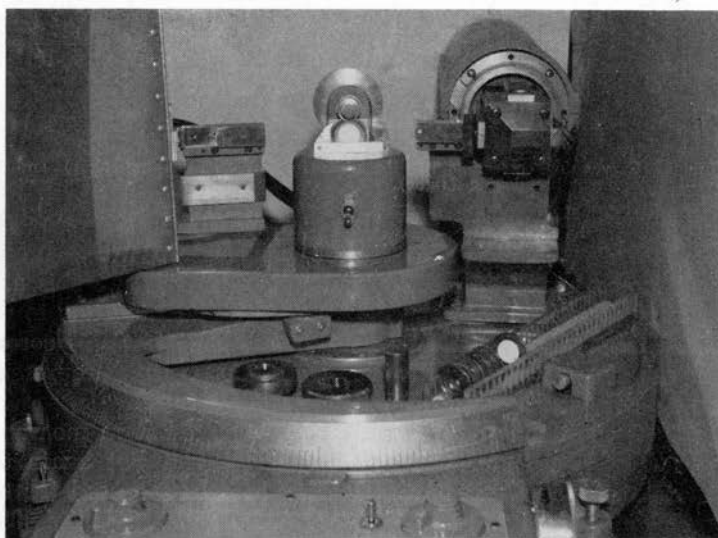


Figure 4. Flat sample spinner, press and disc storage rack.

A small press was then made to pack the samples, and effects of packing pressures were investigated. A pressure of 300 psi was found to be barely sufficient for MgO powder to remain in the holder. Pressures to 1000 psi were tried, and average peak breadth and standard deviations after five repeat runs were calculated and compared. Results are shown in Table 2.

Table 2. Effects of Packing Pressure on Peak Breadth of Untreated MgO Powder

Pressure, psi	$\bar{B}_0^\circ$ (av. of 5)	$\sigma$
300	0.348	0.00147
400	0.351	0.00162
500	0.347*	.....
1000	0.344	0.00286

\* Average of three

Apparently packing pressure has comparatively little effect on  $B_0$ , but high pressures markedly increase the standard deviation,  $\sigma$ . Therefore a pressure of 400 psi was selected, with the

option of higher pressures to retain difficult samples in the holders. Most samples may be freely handled or even dropped without danger of dislodging.

#### Sample Rotation

To increase efficiency further a device was made to continuously rotate the sample disks at approximately 7 rpm in the X-ray beam. Continuous rotation was further found to increase reproducibility and decrease  $\sigma$  materially.

#### Time Constant

The "slow" scan rate of  $0.2^\circ 2\theta$  per minute was used, and the influence of electronic time constant investigated. With an  $0.2^\circ$  detector slit, time constants of up to four seconds did not increase  $B_0$ . However, a minimum of eight seconds was needed to reduce pen jiggle and give good reproducibility, though this increased  $B_0$  about 1.5 percent. A 15-second time constant gave very good reproducibility but increased  $B_0$  about 6.5 percent. The 8-second value was therefore selected.

#### Optics

A  $1^\circ$  beam slit was found to irradiate a proper amount of the  $\frac{3}{8}$ -inch sample and to give a good balance between sufficiently high diffraction intensities and a slim diffraction peak profile.

Use of various detector slits showed that finer slits decreased  $B_0$  but also decreased intensities and reproducibility. Results from samples with 400 psi packing, MR Soller slit, eight second time constant, and intermittent sample rotation are shown in Table 3.

Table 3. Effects of Detector Slit on Peak Breadth of Various Heat-Treated MgO Samples

Sample	Slit width, °	$\bar{B}_0$ , °*	$\sigma$
Coarse (1000° C)	0.05	0.241	0.0034
	0.1	0.250	0.0008
	0.2	0.298	0.0012
Fine (200° C)	0.1	0.370	0.0046
	0.2	0.426	0.0016
V. fine (No treatment)	0.05	0.275	0.0035
	0.2	0.335	0.0023

\* Average of 10 runs.

On the basis of these results the  $0.2^\circ$  detector slit was chosen for fine samples to obtain a low  $\sigma$ , at some sacrifice in resolution. With coarser samples the finer slits also gave low  $\sigma$ , allowing use of a high resolution geometry enabling separation of  $\alpha_1$  and  $\alpha_2$  peaks. The high resolution system incorporates a  $0.02^\circ$  detector slit and HR Soller slit.



### Chart

A chart speed of one inch per minute was selected as convenient, and the linear counts-per-second range was adjusted to give high peaks all on the paper.

### SAMPLES

Crystallite size determinations were made on samples of MgO after various heat treatments previously known to affect size.

Very fine MgO crystallites were prepared by calcining basic magnesium carbonate at a temperature just above the decomposition point. A large sample of Mallinckrodt Magnesium Carbonate AR (approximately  $4 \text{ MgCO}_3 \cdot \text{Mg}(\text{OH})_2 \cdot 4\text{H}_2\text{O}$  and with 0.453 percent maximum limit of impurities) was calcined in a platinum crucible at  $400^\circ\text{C}$  for two hours and allowed to cool. Individual samples of the oxide were then fired at elevated temperatures. A small wire-wound electric furnace was used for temperatures up to  $1000^\circ\text{C}$ ; a silicon carbide resistance furnace, for  $1400^\circ\text{C}$ ; and a gas-fired kiln, for  $1600^\circ\text{C}$ . The firing temperature was held for two hours, after which the samples were cooled and stored in small air-tight polyethylene containers.

### RESULTS AND DISCUSSION

#### *MgO Crystallite Size*

MgO crystallite sizes obtained from X-ray diffraction are shown in Table 4. Sizes range from 27.5 to 11,300 Å, increasing regularly with higher temperature treatment.

X-ray intensity measurements indicate that real crystals are not perfectly geometrical structures but contain lattice imperfections of various types (Buerger, 1960, p. 197). One concept is that a real crystal is composed of a number of smaller units or crystallites, each one having a slightly different orientation. This type of substructure is known as mosaic or lineage structure.

*Electron microscope.* To check on the reliability of the X-ray measurements and to find whether the MgO crystallites occur as discrete particles or in mosaic, several samples were studied by an electron microscope (RCA Model EMU 2A). A very small amount of each sample was placed in a drop of one percent parlodion in amyl acetate and spread to a film between two microscope slides. After the film dried it was scored into approximately three mm squares which were floated off on water and onto small metal grids. Calibration of the microscope was accomplished by using a diffraction grating replica with 28,800 lines per inch.

Table 4. Average Crystallite Size from X-ray Diffraction of Heat-Treated MgO

Treatment °C	$B_0$ , ° $2\theta$	$\sigma$	$\beta$ , ° $2\theta$	$D$ , Å	95% confidence range, Å <sup>2</sup>	
350	3.50	.....	3.4458	27.5		
400	2.634	.2059	2.5696	36.9	35.5 to	38.4
500	1.210	.0005	1.1181	84.8	84.7 to	84.9
600	.7455	.0039	.6216	152.6	152.1 to	153.1
700	.4537	.0025	.2767	342.7	340.7 to	344.9
800	.3415	.0026	.1315	721.3	712.1 to	730.8
900	.3167	.0020	.09821	965.9	951.3 to	980.8
1000	.2937	.0009	.06646	1,427	1401 to	1454
1400	.2918	.0019	.06358	1,492	1458 to	1527
1600	.0899	.0005	.00836	11,300	8390 to	17,500
Ref. Magorite, low resolution	.2491	.0024	0	$\infty$		
Ref. Magorite, high resolution <sup>1</sup>	.0828	.0059	0	$\infty$		

<sup>1</sup> High resolution (0.02° det. slit). All others low resolution (0.2° det. slit).

<sup>2</sup> The range is calculated from 95 percent confidence limits of  $\bar{B}_0$  from ten measurements.

As shown in Figure 5 no well-developed cubic habit is seen, and particles are angular to subangular or prismatic in shape. Particle sizes were measured from the negatives with a 7x comparator, average particle size being taken as  $\sqrt[3]{a \times b^2}$ , where  $a$  was the longer axis and  $b$  the shorter. Results are given in Table 5.

Table 5. Average size of MgO Particles from Electron Micrographs

Treatment, °C	Å
400	37,300
600	41,600
800	43,400
1000	49,000
1600	53,500

The amount of change in particle sizes seen in the electron microscope is much less than the corresponding change in crystallite size by X-ray diffraction, suggesting that in spite of the errors in both methods the crystallites must occur as aggregates or mosaics. This is further substantiated by the obvious aggregate form shown in the micrographs.

*Change in unit cell.* The exceedingly fine crystallite size of low temperature-treated MgO may reflect the change of MgO from an amorphous to a crystalline state. This is further sug-

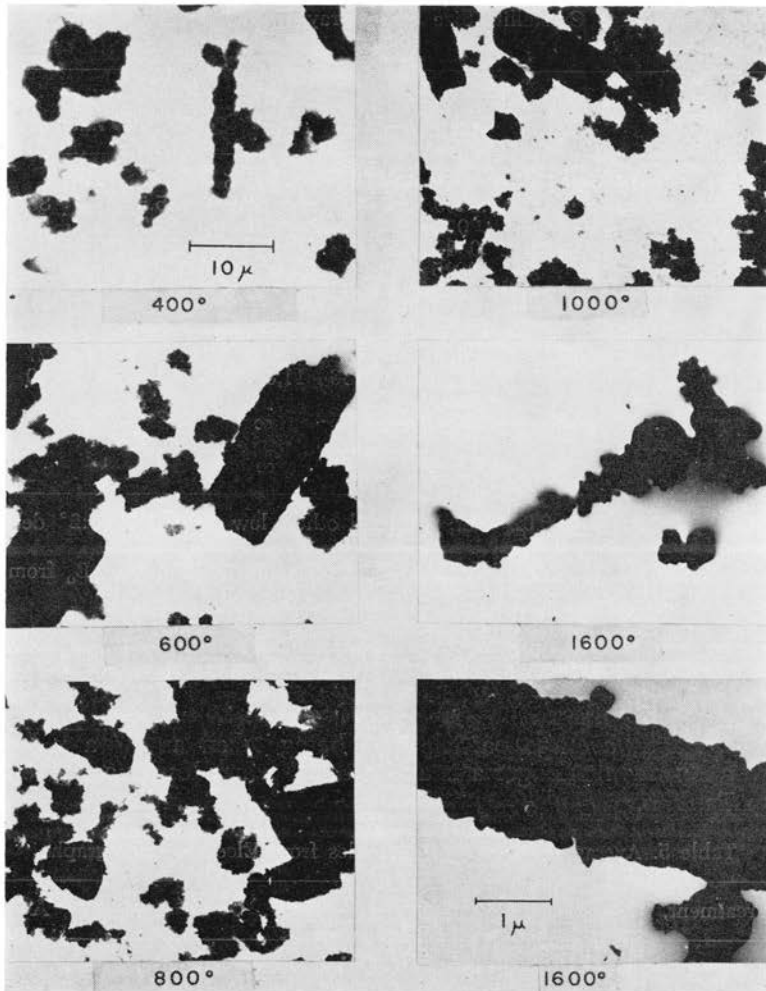


Figure 5. Electron micrographs of heat-treated MgO powder. Scales for all but the lower right are the same as for the 400° treated sample.

gested by change in unit cell obtained through the Bragg equation from  $2\theta$  data on the X-ray diffraction tracings. The unit cell size decreases considerably as temperature of treatment increases, the structure finally becoming orderly and unchanged after about 1000°C (Figure 6). The  $a_0$  dimensions should be regarded as relative due to errors arising from use of a diffractometer for these measurements.

*Particles, crystallites, and unit cells.* Low temperature calcination of basic magnesium carbonate gives an MgO powder, individual particles, which are only about 27

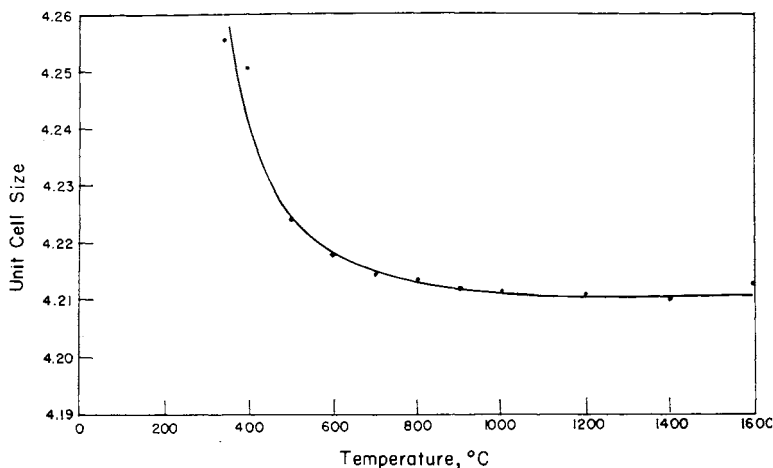


Figure 6. Relation of MgO unit cell size to temperature of treatment. Diffractometer data.

Å or a few unit cells thick. The crystallites have an expanded unit cell and perhaps an imperfect crystal structure which may contribute an unknown amount to line broadening.

Heat treatment to 600°C causes an appreciable tightening of the unit cell and moderate growth of apparent crystallite size. Heat treatment above 600°C results in gross increases in crystallite size coupled with some further tightening of the unit cell which all but ceases at about 1000°. Heating above 1000° further increases the crystallite size but does not change the unit cell size.

The change in crystallite size on heating is accompanied by only a moderate increase in size of the MgO aggregate particles. If both X-ray and electron microscope size data are accepted, in the 400°C treated powder an average aggregate contains about  $\left(\frac{37,300}{36.9}\right)^3 =$  one billion crystallites. In the coarsest powder

so far investigated (1600°C), an average aggregate contains only about 100 of the large crystallites. In terms of surface area of crystallites, the finest powder should have about 400 times the internal surface area of the same weight of the coarsest powder.

*B.E.T. gas adsorption.* Surface areas of three samples of commercially prepared MgO were evaluated by the Brunauer-Emmett-Teller nitrogen gas adsorption method for comparison with the X-ray method. A sample heated to 1000°C measured 8.8 m<sup>2</sup> per gm, which gives an average crystallite dimension of 1100 Å if crystallites are assumed to be cubes. The comparable X-ray

datum is 1427 (range 1415-1440 Å). Of the other two samples, one treated at 1400°C was too coarse to be measured by gas adsorption, and the other had had an indefinite heat treatment. We can conclude from the 1000° sample that a large area of the crystallites is available for nitrogen gas adsorption, even though the crystallites occur as aggregates.

### *The Line Broadening Method*

With ordinary precision, the upper limit of usefulness of the X-ray line-broadening technique is considered to be about 1000 to 2000 Å; in other words, sizes larger than this give a diffraction peak which is uniformly sharp. This limit may be arrived at as follows: with Cu K  $\alpha$  radiation,  $2\theta = 40^\circ$ , and the limit of precision of measurement of  $B_0$  and  $\beta$  taken as  $0.2^\circ$  ( $= 1.146 \times 10^{-3}$  radians),

$$D_{\max} = \frac{1.54 (10)^3}{1.146 \cos 20^\circ} = 1430 \text{ \AA}.$$

Greater precision in the determination of  $\beta$  would allow measurement of coarser sizes.

In the present research  $B_0$  and  $\beta$  were obtained to the nearest  $0.001^\circ$ , and the standard deviation from ten measurements was found to average around  $0.0024^\circ$  (Table 4). The standard deviation of the difference was taken as the square root of the sum of the squares of  $\sigma_B$  and  $\sigma_{\text{ref.}}$ , and averages about  $0.0011^\circ$ , giving 95 percent confidence limits of about  $\pm 0.0005^\circ$ . With this accuracy of measurement the upper limit of size determination may be of the order of 100,000 Å, or ten microns, with an accuracy in this range of about  $\pm 100$  percent.

This limit was not reached in the present research, the maximum size measured being 11,300 with 95 percent confidence limits 8,390 and 17,500 Å. The range is made abnormally high by the high  $\sigma$  for the reference material. If by better size separation of material this  $\sigma$  is reduced to the expected range of  $0.002^\circ$ , the confidence limit range will be reduced about one-half, giving a relative accuracy in the 10,000 Å range of about  $\pm$  five percent.

The lower size limit measurable by the line broadening method is a matter of ability to recognize an extremely low, broad diffraction peak. The lowest value was approached in the finest sample tested, which has a thickness of 27.5 Å, or 6.5 unit cells.

## CONCLUSIONS

The present research indicates

1. Calcination of basic magnesium carbonate at a temperature just above the decomposition point yields an oxide characterized by very coarse aggregates composed of very fine crystallites which are only a few unit cells thick. The unit cells are dilated about one percent compared with higher temperature treated samples.
2. The aggregates increase uniformly in size with increase in temperature up to 1600°C (from about 37,000 to 53,000 Å).
3. Crystallite growth is moderate up to about 600°C (from 27.5 to 152 Å). Above 600°C, crystallite growth is very great (from 152 to 11,300 Å at 1600°C).
4. The unit cell tightens with temperatures up to 1000°C, above which little change was found.
5. B.E.T. gas adsorption data on a 1000°C treated sample correlate closely with crystallite size.
6. The upper limit of measurement of crystallite size by X-ray diffraction may be extended 10 to 100 times, to the size range 10,000 to 100,000 Å, by use of precision diffractometer techniques including proper sample preparation and rotation and by use of statistical treatment.

## ACKNOWLEDGEMENTS

The B.E.T. gas adsorption surface area measurements were obtained through the courtesy of the Wood River Laboratory of the Shell Oil Company, H. Sutherland, Chief Technologist.

Appreciation is expressed to Dr. Thomas McGee of the Department of Ceramic Engineering for use of various ovens in this study, and also to Dr. Evans Roth of the Department of Physics for assistance in obtaining suitable electron micrographs.

## APPENDIX A

CALCULATION OF ANGULAR SEPARATION OF  $\alpha_1$  AND  $\alpha_2$  RADIATION

Data for angular separation of the two components of various K radiations are given in the Internationale Tabellen accurate to two significant figures. A direct calculation using the Bragg relationship

$$\sin \theta_1 = \frac{\lambda \alpha_1}{2d}, \quad (1)$$

$$\sin \theta_2 = \frac{\lambda \alpha_2}{2d}, \quad (2)$$

where  $d$  is crystal spacing and  $\lambda$  is wavelength in Angstroms, is tedious and gives only two or three significant figures, because the two  $\theta$  angles must be subtracted to obtain angular separation.

An equation for small values of  $\Delta \theta$  was developed as follows: Subtracting the above,

$$\frac{\lambda\alpha_2 - \lambda\alpha_1}{2d} = \sin \theta_2 - \sin \theta_1,$$

$$= 2 \sin \frac{1}{2} (\theta_2 - \theta_1) \cos \frac{1}{2} (\theta_2 + \theta_1)$$

$$2 \sin \frac{1}{2} (\theta_2 - \theta_1) = \frac{\lambda\alpha_2 - \lambda\alpha_1}{2d \cos \theta \text{ av}} \quad (3)$$

Substituting  $d = \frac{\lambda \text{ av}}{2 \sin \theta \text{ av}}$

$$2 \sin \frac{1}{2} (\theta_2 - \theta_1) = \frac{\lambda\alpha_2 - \lambda\alpha_1}{\lambda \text{ av}} \tan \theta \text{ av} \quad (4)$$

For very small angles the sin is very nearly equal to the angle in radians,  $2 \sin \frac{1}{2} (\theta_2 - \theta_1) = \theta_2 - \theta_1$ . Expressed in terms of degrees  $2\theta$ ,

$$\Delta = \frac{360}{\pi} \frac{\lambda\alpha_2 - \lambda\alpha_1}{\lambda \text{ av}} \tan \theta \text{ av} \quad (5)$$

$$= C \tan \theta \text{ av} \quad (6)$$

Various values of  $C$  for different X-ray tube targets are given below:

Radiation	C
Cr $K\alpha$	0.195
Fe $K\alpha$	0.233
Co $K\alpha$	0.249
Ni $K\alpha$	0.266
Cu $K\alpha$	0.285
Mo $K\alpha$	0.690
Ag $K\alpha$	0.899

Example: Cu $K\alpha$  radiation  $2\theta_{av} = 42.88^\circ$

$$\Delta = 0.285 \tan 21.44^\circ$$

$$= 0.112^\circ$$

## APPENDIX B

### SAMPLE CALCULATION

Symbols:

$\Delta$  = angular separation of  $\alpha_1$  and  $\alpha_2$  diffraction peaks in terms of degrees.

$B_0$  = measured breadth of diffraction peak at half maximum intensity, degrees  $2\theta$

$B$  =  $B_0$  corrected for  $\alpha_1 \alpha_2$  separation

$\beta$  = diffraction line broadening =  $B$  corrected for instrument broadening

$b_0$  =  $B_0$  for coarse reference material ( $\beta=0$ )

$b$  = instrument broadening =  $b_0$  corrected for  $\alpha_1 \alpha_2$  separation

$D$  = average crystallite size normal to the diffracting planes

$K$  = a constant taken as 1.0

Example: Let

$$\bar{B}_0 = 0.4537^\circ$$

$$\bar{b}_0 = 0.2491^\circ$$

$$\Delta = 0.1120^\circ \text{ (Appendix A)}$$

$$2\theta = 44.88^\circ$$

$$\lambda = 1.54050 \text{ \AA} \text{ (Cu } K\alpha_1\text{)}$$

$$1. \text{ Find } B \text{ from } B_0 : \frac{\Delta}{B_0} = \frac{0.1120}{0.4537} = 0.247$$

$$\text{From the left graph, Figure 3, } \frac{B}{B_0} = 0.9425$$

$$B = 0.4276^\circ$$

$$2. \text{ Similarly, } b = 0.767 \text{ (} b_0 = 0.1911^\circ \text{)}$$

This value remains constant for all similar samples tested by the same diffraction geometry.

$$3. \text{ Find } \beta \text{ from } B \text{ and } b : \frac{b}{B} = \frac{0.1911}{0.4276} = 0.447$$

$$\text{From the right graph, Figure 3, } \frac{\beta}{B} = 0.6470$$

$$\beta = 0.2767$$

4. Calculate  $D$ :

$$D = \frac{K\lambda}{\beta \cos \theta} = \frac{(1.0) (1.54050) (360)}{(0.2767) (0.93080) 2\pi} = 342.7 \text{ \AA}$$

#### Literature Cited

- Buerger, M. J. 1960. J. Wiley & Sons, Inc., New York.  
 Internationale Tabellen zur Bestimmung von Kristallstrukturen, Vol. 2, 1935. Gebrüder Borntraeger, Berlin.  
 Klug, H. P. and Alexander, L. E. 1954. X-ray Diffraction Procedures. John Wiley & Sons, Inc., New York.  
 Scherrer, P. 1918. Göttinger Nachrichten, Band 2, p. 98.